

LARGE SCALE ANALYSIS OF MAMMALIAN AXON GUIDANCE AND NEURON POLARIZATION USING ARRAYS OF MICROFLUIDIC GRADIENT GENERATORS

Nirveek Bhattacharjee and Albert Folch

Department of Bioengineering, University of Washington, Seattle, WA 98195

ABSTRACT

In this paper, we report the development of a large-scale microfluidic gradient generator array for the study of axon growth and guidance dynamics of up to 1024 individual primary mammalian neurons in parallel. We adapt a previously reported microfluidic method of creating gradients on open surfaces termed “microjets” [1]. We combine microjets with live-cell, auto-focus time-lapse imaging to create an integrated platform. This format (a) gives us statistically-rich data from each experiment, (b) produces a stable gradient with negligible shear forces on the culture surface, (c) is amenable to long-term culture of neurons, and (d) allows for the presentation of concentration gradients of two opposing biochemical molecules.

KEYWORDS: Microfluidics, gradient generator, axon guidance, PDMS, primary mammalian neurons

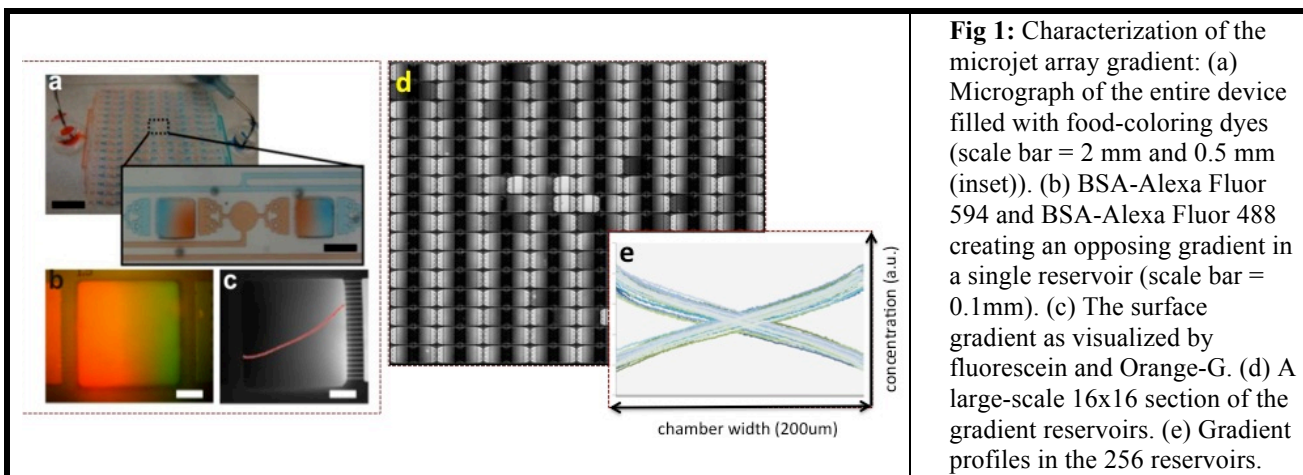
INTRODUCTION

Morphogen and chemokine gradients have been widely implicated in myriad biological phenomena, such as stem-cell differentiation, axonal navigation, cell migration, and immune response [1]. However the difficulty associated with manipulating these intricate processes in vivo motivates the development of high-throughput platforms that can present precisely controlled gradients of diffusible biochemical cues to isolated individual cells and track their response real-time. We have previously described a method for generating steady-state gradients on open surfaces [2], in which it is possible to expose axons to a gradient of a diffusible biomolecule, with negligible shear imparted on the cultured cells [3]. However, in order to ensure that the axonal dynamics we observe is necessarily and sufficiently a response to the externally applied gradient of a biomolecule, it was imperative that we created single-neuron microfluidic gradient chambers. To achieve this, we have implemented a parallel array of single cell microfluidic gradient generators.

EXPERIMENTAL METHODS

The microfluidic gradient generator array is fabricated by contact-transferring a 250 μm poly(dimethylsiloxane) (PDMS) micro-structure, “exclusion-molded” off a master template created using multi-layer standard SU-8 photolithography on silicon wafers, as described earlier [2]. Each unit of the array, henceforth called the gradient chamber, is 250 μm high, 200 μm wide and 400 μm long, and is fed on each side by a row of microjets, 2 μm high and 10 μm wide (Fig 1a). The gradient chambers are 1.2 mm apart, resulting in a 16x64 rectangular array. The cured PDMS membrane after being picked up from the silicon master, with a fluoro-polymer backed mylar sheet (3M Scotchpak Release Liner 9744), is plasma bonded to a glass cover-slide [2].

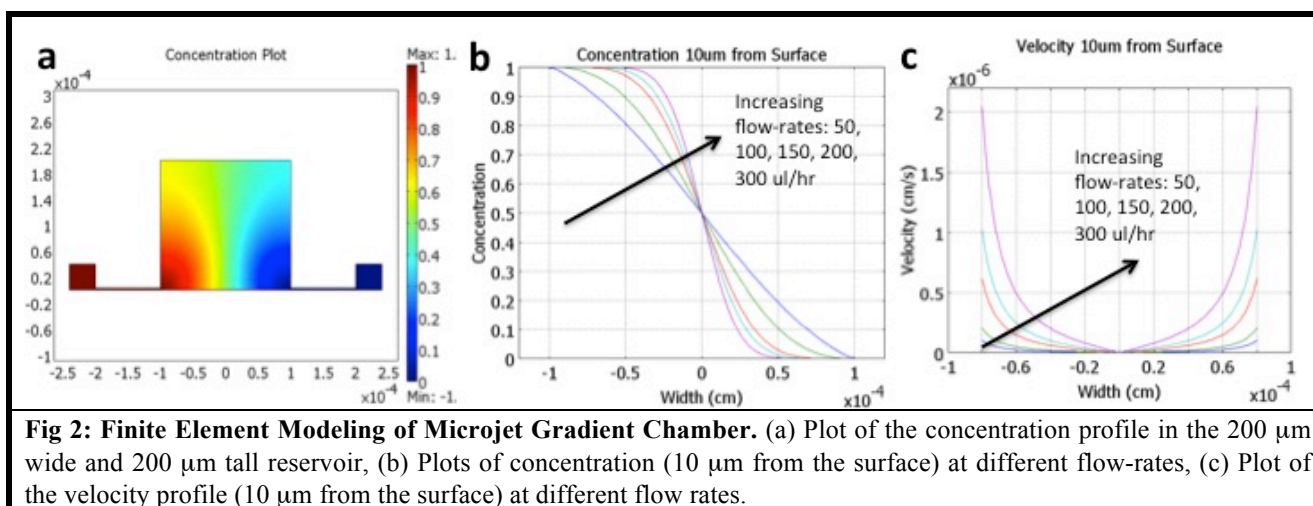
After the assembly, characterization and sterilization of the devices, dissociated neurons from E18 mouse hippocampus (12,000 cells/mL) are allowed to settle onto the device, the surface of which is pre-coated with polylysine (50 $\mu\text{g}/\text{mL}$, 1 hour) and laminin (5 $\mu\text{g}/\text{mL}$, 8 hours). The cells are cultured in the chambers for 24 hours (in case of axon guidance studies), or 2 hours (in case of axon specification studies). For the axon guidance studies we interrogated the neurons with a gradient of netrin (200 ng/mL on one end and media on the other), which resulted in a linear gradient across the 200 μm width of the chamber, for 6-12 hours. We used trace amounts of fluorescent-BSA to visualize the gradient. For the axon-specification studies, we presented the cultured neurons with a gradient of 8-Sp-Br-cAMP (a cell-



permeable analog of cyclic AMP) at 20 $\mu\text{g}/\text{mL}$ and maintained the gradient for 18-24 hours. In both cases, we obtained time-lapse images every 15 minutes, using a TE-2000 Nikon inverted epi-fluorescence microscope.

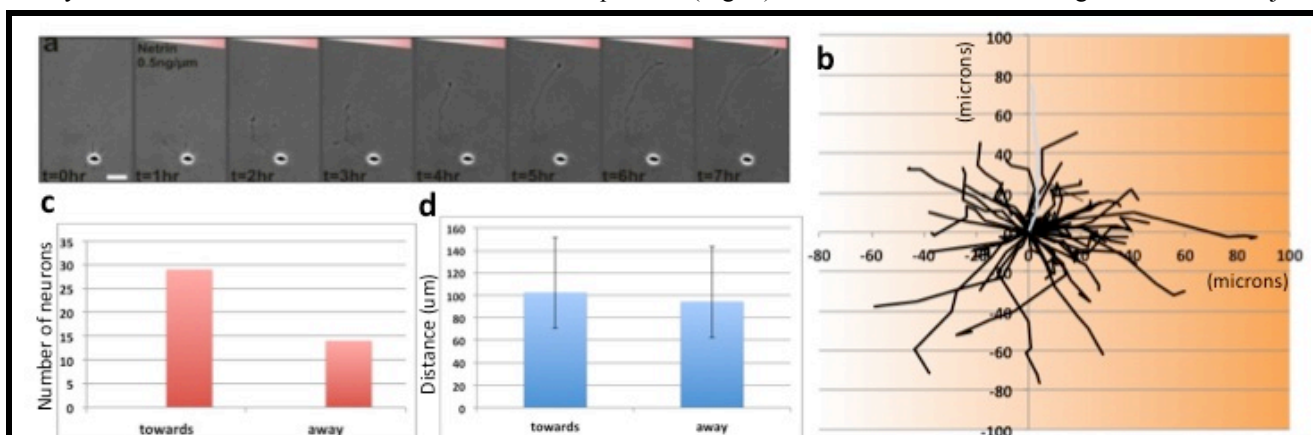
RESULTS AND DISCUSSION

The gradient in the chambers is visualized with 10 mM red and blue food coloring dyes (as shown in Fig 1(a), and the corresponding higher magnification inset). The gradient is established within 5 minutes of initiating flow through the microjets in the device. The shape and profile of the gradient can be altered by modulating the pressure heads (or the flow rate, if using syringe pump) driving the flow in the two sets of microjets. Unlike in most microfluidic gradient generators, in our device the gradient is primarily created by convection (i.e. the effect of diffusional transport is negligible). Therefore, the resulting concentration profile is independent of the molecular weight of the species, which allows us to use tracer molecules to visualize the gradient. In Fig 1(b), we use fluorescently labeled bovine serum albumin (BSA) to visualize the gradient, and the profile appears similar to the food coloring dyes.



We used a previously described method based on Beer-Lambert law [4] to measure the surface gradient in the chambers (Fig 1c), which is a more accurate indication of what the cells sense. In order to visualize the surface gradient, 1 mM fluorescein mixed with 45 mM Orange G was flowed through one set of microjets, while the bath, chambers and the other set of microjets was filled with 45 mM Orange G. The protocol utilizes the light absorption spectrum of Orange-G, a non-fluorescent dye that absorbs energy strongly at the excitation wavelength (490 nm) of the dye (fluorescein), but weakly at its emission wavelength (540 nm). Orange-G competes with fluorescein in solution for excitation energy; at 45 mM (with a 0.6 NA objective), it results in an effective penetration length of $\sim 4.9\mu\text{m}$ for fluorescein [4]. Since the excitation decays exponentially from the surface, 95% ($0.95 \approx 1 - 1/e^3$) of the fluorescence intensity that we detect comes from the volume that is within $\sim 15\mu\text{m}$ of the surface. The slope of the surface gradient formed in our 1000 chamber device (Fig. 1d) is spatially and temporally consistent and repeatable, that is, the slope is invariant over time and across chambers (Fig. 1e).

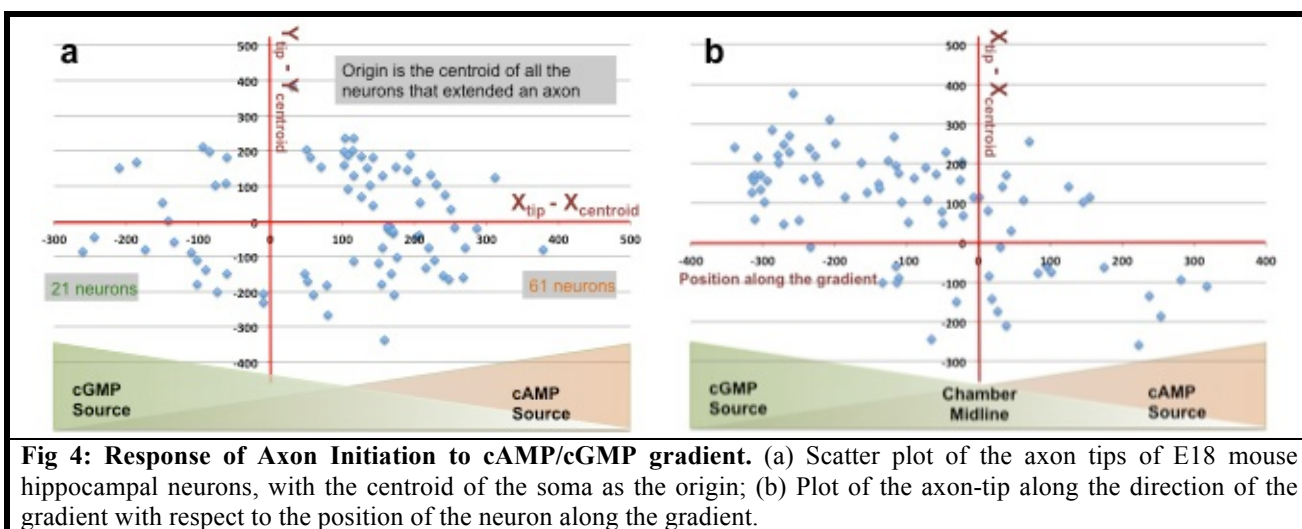
We used finite-element modeling (COMSOL 3.5a) to simulate the flow velocity and concentration profiles using steady-state Navier-Stokes and convection-diffusion equations (Fig. 2). The flow lines after coming out of the microjets



primarily traverse vertically, with a small horizontal component, which is enough to create the concentration gradient in the horizontal direction (Fig. 2a). We found an optimum flow rate that can create a linear gradient across the entire width of the chamber (Fig. 2b) as well as ensure that the shear stresses on the cells in the device (which is proportional to the horizontal component of the flow-velocity next to the surface) are minimal (Fig. 2c). Due to the small horizontal component of the flow velocity, there is very little shear stress on the surface, making this class of devices very benign to long-term culture of neurons [2].

We used this device for the first time to look at guidance dynamics in over 100 neurons at the same time, under the same precise gradient conditions. The neurons were exposed to gradients after 24 hours of plating, when most of the neurons have extended a prominent neurite. As is evident in the micrographs below (Fig. 3a) hippocampal axons were shown to turn towards the source of netrin gradient. We combined the trajectories of the neurons that extended axons by over $30\mu\text{m}$ during the course of gradient application (Fig. 3b). We found that there were two times more neurons that turned towards the gradient than away from the gradient (29 turned towards, whereas 14 turned away from the gradient). The responding neurons were mostly in a narrow concentration window of 70-140 ng/mL (Fig. 3c).

In addition, we also looked at how opposing gradients of cAMP and cGMP played a role in determining axon initiation by exposing neurons to gradients when the neurons had not yet extended neurites. The cumulative scatter plot (Fig. 4a) of the axon tips shows that there are thrice as many neurons that extend axons towards the higher cAMP side of the chamber. Furthermore, if we plot the extension of the axons towards the gradient (by measuring the difference between the x-coordinates of the axon-tip and the soma-centroid) with respect to the position of the neuron along the gradient, we observe that most of the neurons (~80%) that extend axons towards the cAMP side, are on the lower-cAMP/higher-cGMP end of the chamber (Fig. 4b). This significantly biased response might be due to the fact that the percent change of concentration of a species across the width of a cell, in the lower concentration end of a linear gradient, is higher than the other end.



CONCLUSION

We have shown the proof-of-principle demonstration of a 16×64 parallel array of open-access, microfluidic chambers capable of studying gradient sensing in single neurons. Using this high-throughput platform, the available dataset per experiment is an order of magnitude more than the standard pipette-based techniques. The simplicity and cell-benign nature of this device offers the biological research community a very versatile, enabling high-throughput platform to conduct parallel studies on individual cells that get activated by a chemokine gradient, such as stem-cell differentiation in response to morphogen gradients, cell migration in cancer metastasis, wound repair or immune response.

REFERENCES

- [1] "Biomolecular gradients in cell culture systems", T. M. Keenan and A. Folch, *Lab on a Chip*, 2008, **8**, 34-57 (2008).
- [2] "A neuron-benign microfluidic gradient generator for studying the growth of mammalian neurons towards axon guidance factors", N. Bhattacharjee, N. Li, A. Folch, *Transducers 2009 Conference Proceedings*, 765-68 (2009).
- [3] "Microfluidic jets for generating steady-state gradients of soluble molecules on open surfaces", T.M. Keenan, C-H Hsu, A. Folch, *Applied Physics Letters*, **89**, 114103 (2006).
- [4] "Measurement of the Surface Concentration for Bioassay Kinetics in Microchannels", A. Bancaud, G. Wagner, K.D. Dorfman, J-L Viovy, *Analytical Chemistry* **77**(3): 833-39 (2005).